Angewandte Chemie International Edition

Angewandte International Edition Chemie

GDCh German Chemical Society

How to cite: *Angew. Chem. Int. Ed.* **2026**, e17752
doi.org/10.1002/anie.202517752

COMMUNICATION OPEN ACCESS

Hydrophilic Janus Micelles From an ABC Triblock Copolymer

José Muñoz-López[1,2] | Lei Hu[1,2,3] | Hui Wang[4] | Xiaohe Tian[3,5] | Lorena Ruiz-Pérez[1,6] | Giuseppe Battaglia[1,7]

[1]Institute for Bioengineering of Catalonia (IBEC), The Barcelona Institute of Science and Technology, Barcelona, Spain | [2]Department of Inorganic and Organic Chemistry, Faculty of Chemistry, University of Barcelona, Barcelona, Spain | [3]Functional and Molecular Imaging Key Laboratory of Sichuan Province, Huaxi MR Research Centre (HMRRC), Department of Radiology, and Laboratory of Aging Research and Cancer Drug Target, State Key Laboratory of Biotherapy and Cancer Center and National Clinical Research Center For Geriatrics, West China Hospital of Sichuan University, Chengdu, China | [4]School of Pharmacy, Wannan Medical College, Wuhu, China | [5]Huaxi Xiamen Institute of Medical Research and The Xiamen Key Laboratory of Psychoradiology and Neuromodulation, West China Xiamen Hospital of Sichuan University, Xiamen, Fujian, China | [6]Serra Hunter Fellow, Department of Applied Physics, Faculty of Physics, University of Barcelona, Barcelona, Spain | [7]Institució Catalana de Recerca i Estudis Avançats (ICREA), Barcelona, Spain

Correspondence: Giuseppe Battaglia (gbattaglia@ibecbarcelona.eu)

Received: 12 August 2025 | **Revised:** 28 January 2026 | **Accepted:** 29 January 2026

Keywords: amphiphilic copolymers | Janus particles | poly(ethylene glycol) (PEG) | poly(lactide) (PLA) | poly(*N*-vinylpyrrolidone) (PVP)

ABSTRACT

We describe the creation of an amphiphilic triblock copolymer that drives lateral phase separation within micelle coronas. The design combines a hydrophobic poly(lactide) (PLA) core-forming block with two distinct hydrophilic segments: poly(ethylene glycol) (PEG) and poly(*N*-vinylpyrrolidone) (PVP). In water, the copolymer assembles into spherical micelles, confirmed by cryogenic TEM and multi-angle light scattering. Selective end-labelling of PVP with an electron-dense iridium complex enabled unstained TEM imaging, revealing clear contrast asymmetry that locates PVP to a single hemisphere of the corona. Complementary 2D ^{1}H-Nuclear Overhauser Effect Spectroscopy (^{1}H-NOESY) NMR confirmed this Janus-type segregation of PEG and PVP. These results demonstrate how molecular architecture can encode asymmetry into soft nanostructures, offering a versatile route to polymer-based Janus nanoparticles with dual surface functionality and broad technological potential.

Polymeric Janus nanoparticles are self-assembled structures characterized by two chemically distinct faces. These anisotropic architectures have emerged as powerful platforms in materials science, with potential applications ranging from photonics to targeted biomedical delivery [1, 2]. Among various preparatory strategies, Janus micelles (JMc) may be formed from ABC triblock copolymers, wherein the central B block is insoluble in a specified solvent, while the terminal A and C blocks are soluble. However, achieving a well-defined lateral phase separation of the corona into distinct domains remains a major challenge, regardless of the preparation method [2]. Such a challenge stems from the incomplete phase separation between the corona blocks, resulting in patchy or mixed surface topologies [3]. Lateral segregation of the A and C blocks typically requires that the repulsive interaction, quantified by the Flory–Huggins interaction parameter, χ_{AC}, exceeds a critical threshold. Only when this enthalpy driving force sufficiently outweighs the entropic cost of mixing can distinct Janus-like phase separation in the corona be reliably achieved [4]. Such strong repulsive interactions between corona blocks are readily achieved when one block is hydrophilic and the other hydrophobic, as in the case of amphiphilic Janus micelles. In contrast, Janus micelles with fully hydrophilic coronas, where lateral phase separation occurs between two water-soluble blocks, remain scarcely reported [3, 5]. Herein, we describe the synthesis of an ABC triblock copolymer composed of poly(ethylene oxide)-*block*-poly(lactide)-*block*-poly(*N*-vinylpyrrolidone) (PEG-*b*-PLA-*b*-PVP) and its solvent-switch-driven self-assembly into well-defined Janus micelles. Remarkably, the two hydrophilic

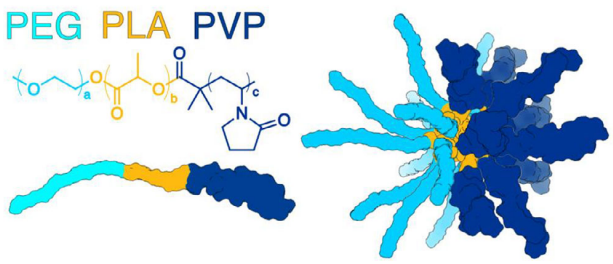

SCHEME 1 | Schematic representation of the self-assembled nanostructure formed by the PEG-PLA-PVP triblock copolymer. Lateral phase separation of the PEG and PVP corona blocks gives rise to hydrophilic Janus nanoparticles with potential for bifunctional surface design.

blocks, PEG and PVP, undergo lateral phase separation in the micellar corona, giving rise to hydrophilic Janus micelles with a chemically asymmetrical surface. This asymmetry introduces unique potential for the design of bifunctional nanoparticles, as illustrated in Scheme 1.

For the synthesis of the triblock, we devised a synthetic route consisting of two steps (Scheme 2). The first step involved the preparation of a poly(ethylene glycol)-*block*-poly(lactide) (PEG-PLA-Br) macroinitiator **3**. This was achieved *via* ring-opening polymerization (ROP) of DL-lactide **1** using α-methoxy-ω-hydroxy poly(ethylene glycol) **2** as the initiator, in the presence of DBU as catalyst. Subsequently, the hydroxyl end-group of the resulting diblock copolymer was esterified with α-bromo-isobutyryl bromide to introduce an atom transfer radical polymerization (ATRP) initiating group. In the second step, *N*-vinylpyrrolidone (NVP) monomer **4** was polymerized using the ω-bromo-functionalized PEG-*b*-PLA macroinitiator **3**. This polymerization was carried out using an in situ generated copper (I) complex with 5,5,7,12,12,14-hexamethyl-1,4,8,11-tetraazacyclotetradecane (Me_6Cyclam) as the ligand. The resulting PEG_{114}-*b*-PLA_{48}-*b*-PVP_{21} triblock copolymer **5** was characterized by gel permeation chromatography (GPC), which revealed a successful chain extension of the PEG_{114}-*b*-PLA_{48} starting polymer (Figure 1B). ^{1}H-NMR spectroscopy, supported by heteronuclear single quantum coherence spectroscopy (HSQC) correlation, confirmed the presence of all three block segments and the full characterization of the triblock copolymer structure (Figure 1A). Furthermore, diffusion-ordered spectroscopy (DOSY) revealed a single diffusion coefficient for all resonances (Figure 1C), verifying that the three blocks are covalently linked and exist as a single macromolecular species.

A triblock copolymer functionalized with an iridium(III) complex **10** was also synthesized as a structural probe to assess the compositional asymmetry of the assembled JNPs (scheme 3). The synthesis began with the preparation of the alkyne-functionalized iridium(III) complex **8**. Starting from the μ-chloro-bridged diiridium precursor **6** [6], the compound was reacted with 1,10-phenanthrolin-4-ol in a mixture of dichloromethane and methanol under an inert atmosphere. These conditions promoted dimer cleavage and ligand substitution, yielding the mononuclear Ir(III) complex **7**. Subsequent alkylation of the phenanthroline hydroxyl group with 3-bromo-1-propyne afforded the alkyne-functionalized complex **8**. In parallel, the bromine-terminated triblock copolymer **5** was converted into its azide derivative **9** by treatment with sodium azide in dimethylformamide at room temperature for 48 h [7]. Without further purification, the resulting azide-functionalized polymer was reacted with complex **8** via copper-catalyzed azide-alkyne cycloaddition (CuAAC) [8], yielding a yellow iridium-conjugated triblock copolymer **10**. Structure characterization and conjugation efficacy were determined by ^{1}H-NMR ($\eta = 52\%$) and GPC. Once both the unmodified and Ir-conjugated triblock copolymer structures were fully characterized, we evaluated their ability to self-assemble into micelles and examined their morphology. Micelles made of PEG_{114}-*b*-PLA_{40} diblock copolymer were used as a control of spherical morphology, as they share the same hydrophilic-to-hydrophobic ratio as the triblock systems. For all samples, micelle formation was induced by solvent switch [9], in which copolymers were dissolved in DMF and then gradually injected into water with a syringe pump at a constant rate. The organic solvent was subsequently removed by dialysis against water to yield the final micellar dispersions.

Dynamic light scattering (DLS) measurements revealed the formation of narrowly dispersed nanoparticles (Figure 2A). The unmodified and Ir-conjugated triblock micelles exhibited average hydrodynamic radii (R_h) of 15.2 ± 6.6 and 21.0 ± 7.8 nm, respectively, indicating that Ir-conjugation had only a modest effect on particle size. In contrast, PEG_{114}-*b*-PLA_{40} micelles displayed a significantly smaller average hydrodynamic radius of 7.2 ± 2.1 nm. A quantitative TEM analysis based on statistically meaningful particle counts (Figure S8) confirms a substantially larger characteristic size for triblock micelles while also revealing a broad size distribution consistent with anisotropic, non-spherical assemblies. Notably, PEG and PVP create two distinct sides on the hydrophobic corona of the micelle, which only allows a bridge-like conformation for the PLA. Similar arrangements have been observed in polymersomes made of poly(ethylene glycol)-*block*-poly(2-(diisopropylamino)ethyl methacrylate)-*block*-poly(2-methacryloyloxyethyl phosphorylcholine) (PEG-*b*-PDPA-*b*-PMPC) [10] and poly(2-methacryloyloxyethyl phosphorylcholine)-*block*-poly(2-(diisopropylamino)ethyl methacrylate)-*block*-poly(*N*,*N*'-dimethyl acrylamide) (PMPC-*b*-PDPA-*b*-PDMA) and partially in poly(ethylene glycol)-b-polybutylene glygcol)-b-poly(ethylene glycol) (PEG-b-PBG-PEG) triblock copolymers [11] (add ref 12). To further investigate micelle morphology, we employed multi-angle light scattering (MALS) to determine micelle aggregation number and analyzed the angular dependence of the scattering intensity using Guinier plots. From these, we can calculate the aggregation numbers of the two micelle types: ~77 chains per micelle for the triblock and ~89 for the diblock. This near-invariant behavior is consistent with previous observations in PEG-*b*-PLA micelle libraries prepared via solvent switch, where maintaining a constant hydrophilic-to-hydrophobic block ratio leads to essentially unchanged aggregation numbers [13]. As shown in Figure 2B, diblock and triblock copolymer micelles exhibit distinct scattering trends at comparable scattering vectors. The Guinier plot for the diblock micelle is highly linear, consistent with isotropic scattering from a compact, spherical morphology [14, 15]. The triblock micelle shows a clear deviation from linearity at higher q^2, suggesting anisotropic scattering likely due to a more complex morphology. The radius of gyration (R_g) was

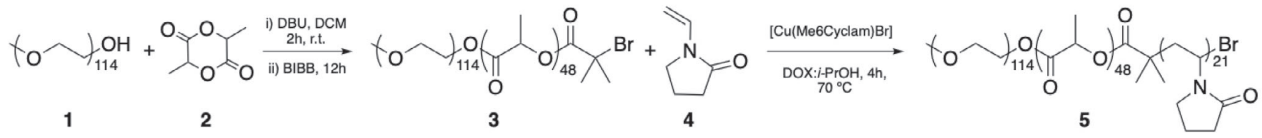

SCHEME 2 | Synthesis pathway of PEG-*b*-PLA-*b*-PVP triblock copolymer. The synthesis involves two steps: (1) ring-opening polymerization (ROP) of DL-lactide initiated by poly(ethylene glycol) (PEG), followed by esterification to obtain the PEG-*b*-PLA-Br macroinitiator; (2) atom transfer radical polymerization (ATRP) of *N*-vinylpyrrolidone (NVP) to yield the final PEG-*b*-PLA-*b*-PVP triblock copolymer.

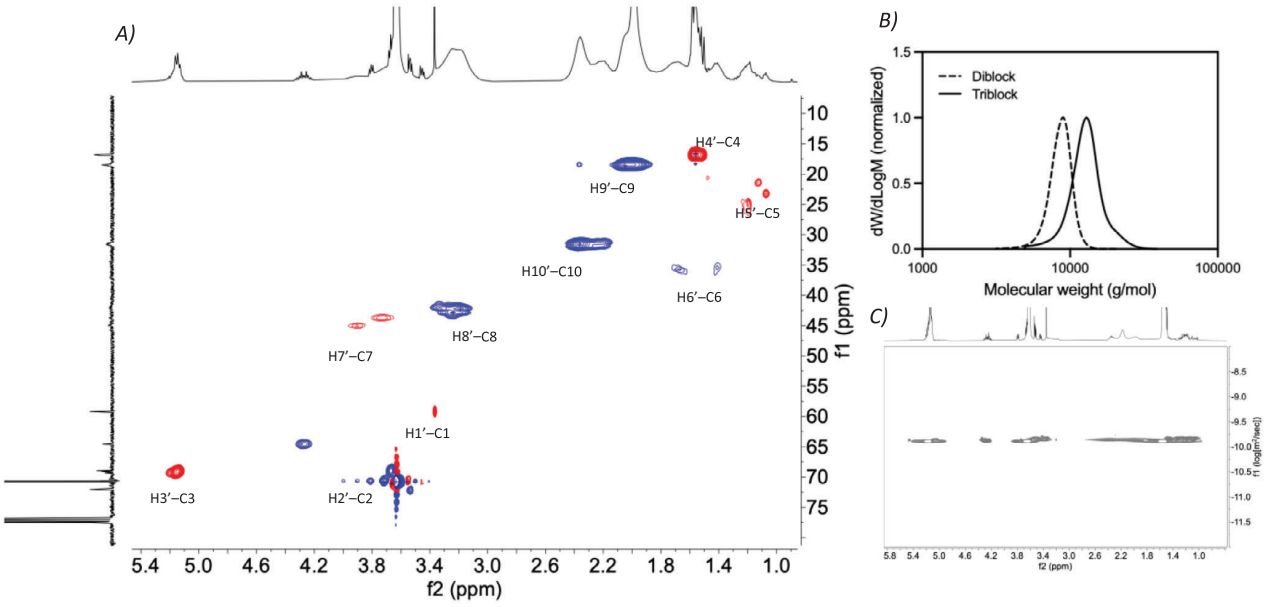

FIGURE 1 | Structural characterization of PEG-PLA-PVP triblock copolymer. (A) Heteronuclear single quantum coherence (HSQC) NMR spectrum of PEG-PLA-PVP. Red signals correspond to methine and methyl groups, while blue signals indicate methylene protons. (B) Gel permeation chromatography (GPC) traces showing the molecular weight distribution of PEG-PLA diblock and the final PEG-PLA-PVP triblock copolymer, confirming successful chain extension. (C) Diffusion-ordered spectroscopy (DOSY) NMR demonstrating a single diffusion coefficient for all three segments, supporting the covalent linkage of PEG, PLA, and PVP blocks within the triblock copolymer.

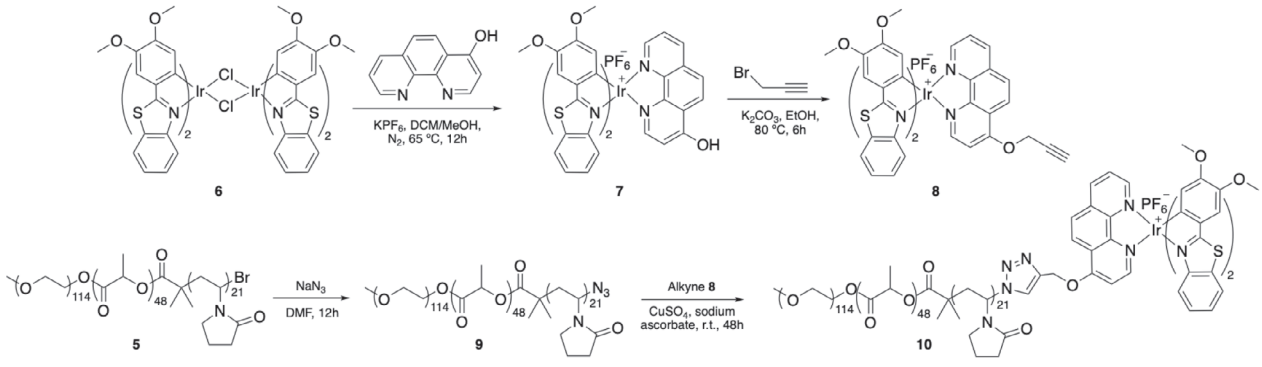

SCHEME 3 | (Above) Synthesis of the Ir(III)–alkyne complex. (Below) One-pot azide functionalization of the PEG-*b*-PLA-*b*-PVP triblock copolymer, followed by conjugation with the Ir(III)–alkyne complex via copper-catalyzed cycloaddition.

determined from the linear regions of Guinier plots for both triblock and diblock micelles. The resulting shape factors (R_g/R_h) for the PEG_{114}-*b*-PLA_{40} diblock micelles were 0.72, in close agreement with the expected value of 0.775 for compact, densely packed spherical structures [16]. The triblock micelles displayed a considerably higher R_g/R_h ratio of 2.0, markedly exceeding previously reported values [17], suggesting a highly asymmetric structure. Cryogenic transmission electron microscopy (Cryo-TEM) confirmed the self-assembly of the PEG-PLA diblock copolymer into spherical micelles (Figure 2C). The triblock

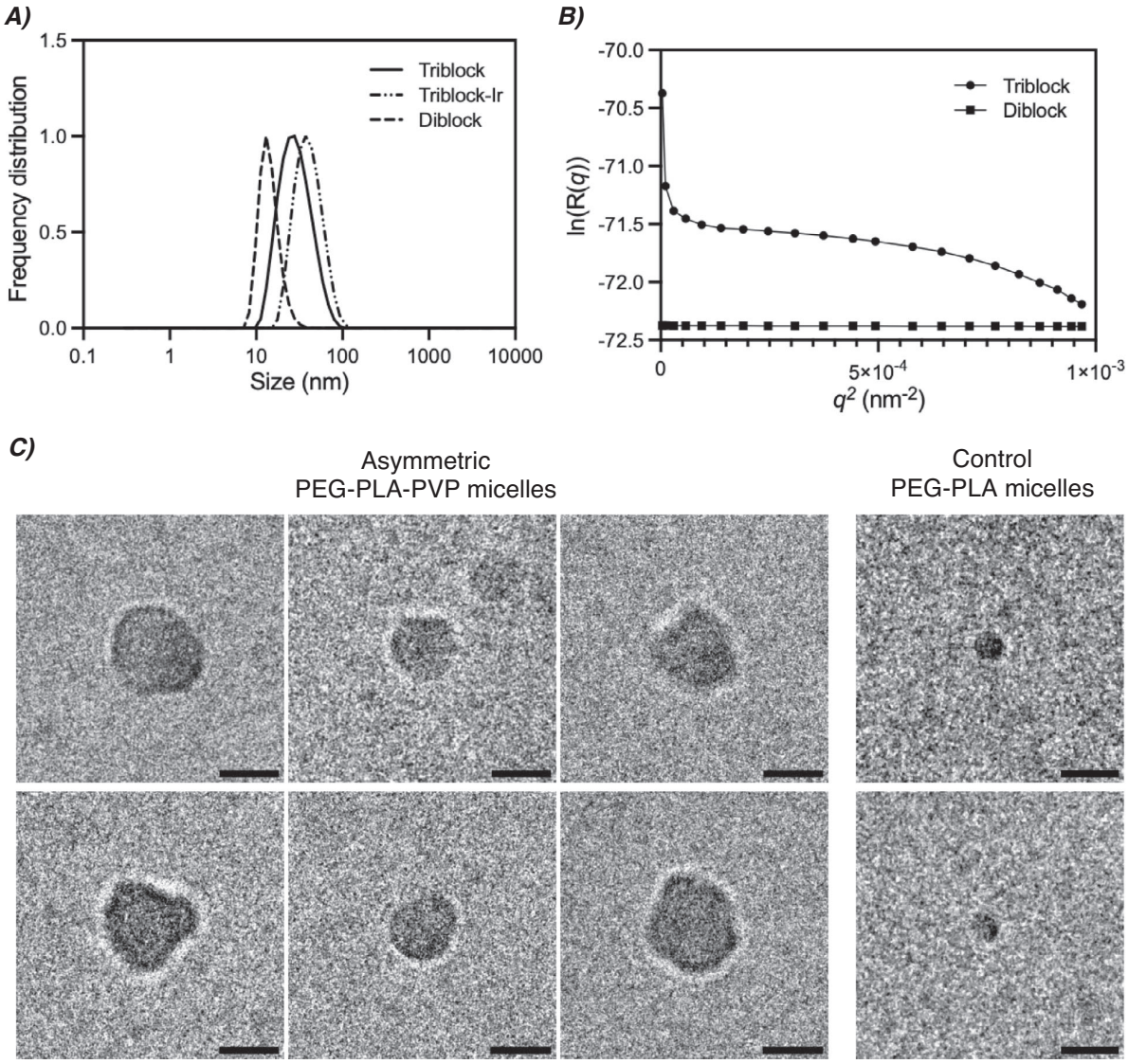

FIGURE 2 | Characterization of PEG-*b*-PLA-*b*-PVP triblock copolymer self-assemblies. (A) Dynamic light scattering (DLS) measurements comparing the hydrodynamic sizes of PEG-*b*-PLA diblock and both PEG-*b*-PLA-*b*-PVP **5** and PEG-*b*-PLA-*b*-PVP-Ir(III) triblock micelles **10**. (B) Guinier plots of control diblock and triblock micelles. The absence of linearity across the scattering vector range of the triblock micelle suggests an anisotropic scattering behavior. (C) Cryogenic transmission electron micrographs of unstained PEG-*b*-PLA and PEG-*b*-PLA-*b*-PVP micelles. Scale bars are 30 nm.

copolymer **5** forms distinctly asymmetric nanostructures, as shown by cryoTEM. Taken together with the comparable aggregation numbers, these results indicate that the diblock copolymer adopts a more compact, coiled PLA conformation within the core, whereas the triblock requires a more extended PLA configuration to incorporate a similar number of chains. The asymmetry observed in the triblock micelles likely arises from the unequal lengths of the two hydrophilic blocks. However, the exact spatial distribution of PEG and PVP within the corona remains undetermined. A multicompartmental organization of the hydrophilic domains may also contribute to the observed asymmetry, giving rise to morphologies that resemble Janus micelles in shape but differ substantially in their internal composition.

Three-dimensional spatial correlations between protons within the triblock copolymer **5** in the self-assembled micelle can offer valuable insight into the degree of segregation between the hydrophilic blocks in the micelle corona. To evaluate whether the corona-forming polymers adopt a mixed configuration, that is, are in close spatial proximity (<0.5 nm), two-dimensional ^{1}H-Nuclear Overhauser Effect Spectroscopy (2D ^{1}H-NOESY) was employed. Symmetric off-diagonal cross-peaks between protons from different blocks would indicate dipolar interactions arising from spatial proximity, consistent with a partially or fully mixed corona [18, 19]. As illustrated in Figure 3A, several cross-peaks are observed, including intramolecular correlations (green and blue) that correspond to dipolar interactions between protons within the same polymer block, as well as intermolecular correlations (purple), which indicate close spatial contacts between protons of different blocks. The cross-peaks encircled in green originate from intramolecular correlations between methine and methylene protons within the PLA block. Conversely, the blue-encircled cross-peaks represent intramolecular interactions within the PVP

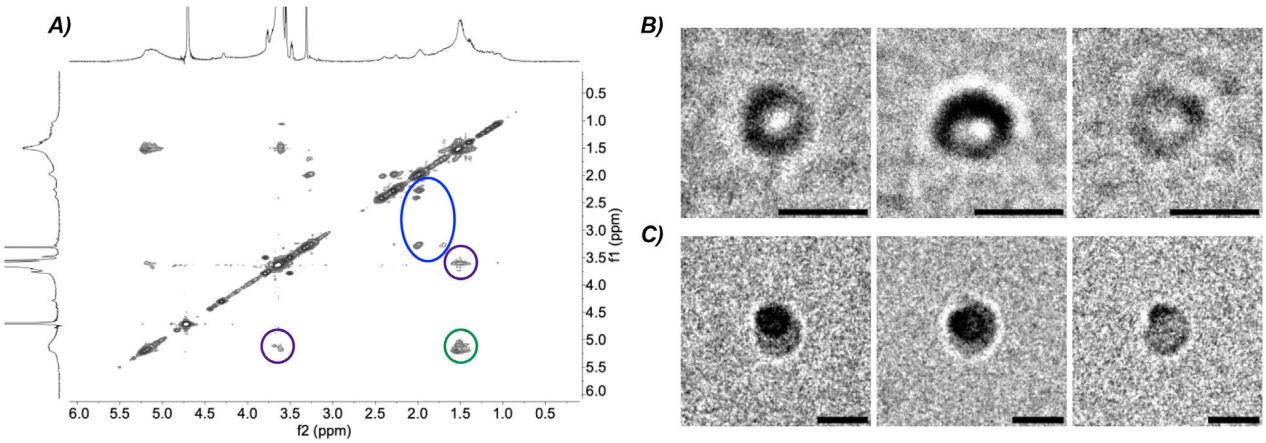

FIGURE 3 | Characterization of lateral phase segregation of PEG-PLA-PVP triblock copolymer micelles. (A) Two-dimensional ^{1}H-Nuclear Overhauser Effect Spectroscopy (2D ^{1}H-NOESY) of micelles formed by the self-assembly of PEG-PLA-PVP **5** in D_2O. The absence of cross-peaks between PEG and PVP proton signals indicates minimal spatial proximity between the two blocks, suggesting a high degree of lateral phase segregation within the micellar corona. (B) Transmission electron and (C) cryogenic transmission micrographs of unstained the iridium-conjugated PEG-PLA-PVP triblock **10** micelles. The observed contrast asymmetry along the micelle periphery suggests a laterally segregated corona arising from spatial separation of the hydrophilic PEG and PVP blocks. Scale bars are 30 nm.

block, involving methylene protons of the pyrrolidone ring and potentially contacts with protons along the polymer backbone. In contrast, the purple-encircled cross-peaks denote intermolecular correlations between PEG and PLA blocks, suggesting close spatial proximity at the micelle interface. Significantly, no cross-peaks are observed between the PVP and PLA blocks, indicating a reduced interfacial contact. This observation supports a model in which PEG chains adopt a more coiled conformation near the micelle interface, consistent with previous molecular dynamics simulations of PEG-*b*-PLGA [20] and PEG-*b*-PLA micelles [13]. In contrast, PVP chains, likely due to their shorter length and steric hindrance from the pyrrolidone rings, adopt a more extended conformation. The absence of cross-peaks between the two hydrophilic blocks, PEG and PVP, further suggests a high degree of phase segregation between them.

Transmission electron microscopy (TEM) and cryo-TEM analyses were performed on unstained micelles formed from the Ir-conjugated triblock copolymer **10**. As shown in Figure 3B, the micelles exhibit pronounced contrast asymmetry, with one hemisphere appearing significantly darker. This differential contrast arises from the electron-dense iridium label, which is selectively positioned at the PVP chain end, providing direct visual evidence for the spatial confinement of the PVP block to one side of the micelle surface. Complementary cryo-TEM images (Figure 3C) offer a more faithful representation of the micelle morphology in solution. The apparent difference in the extent of Ir(III)-rich regions between Figure 3B,C can be attributed to differences in micelle orientation relative to the electron beam and to beam-induced effects. In Figure 3B, the micelles are primarily oriented *face-on*, causing multiple Ir-tagged pop chain ends to overlap in projection; combined with a higher electron dose, this produces a broad dark region surrounding a brighter, partially eroded center. In contrast, micelles in Figure 3C are viewed at an angle and imaged at a lower dose, resulting in discrete, smaller dark spots corresponding to individual Ir-labeled chain ends.

Furthermore, the variation in the size of the dark regions observed across the micrographs in Figure 2C is consistent with the conjugation efficiency of the Ir(III) tag (~52%), meaning that uniform Ir(III) labeling across all micelles is not expected. The consistent localization of contrast across both TEM and cryo-TEM strongly supports a laterally segregated corona architecture. This observation is consistent with the absence of NOE cross-peaks between PEG and PVP domains, indicating minimal spatial overlap between the two hydrophilic blocks. In addition, the similar morphologies observed by cryoTEM for both Ir(III)-tagged and untagged micelles confirm that the Ir(III) end group does not significantly influence polymer self-assembly. Taken together, these complementary findings support the formation of a Janus-type micelle, characterized by a phase-separated corona in which PEG and PVP are compartmentalized into distinct hemispherical regions.

In our recent study [13], we systematically investigated a library of PEG–*b*-PLA diblock copolymers with a fixed hydrophilic-to-hydrophobic ratio and demonstrated that the PLA block in diblock micelles adopts a compact conformation consistent with a worm-like chain in the flexible regime. As a consequence, the micelle radius shows a markedly weaker dependence on molecular weight than predicted by classical core–shell models that assume a fully stretched hydrophobic core, leading to diblock micelles that are significantly smaller than expected. In contrast, the PEG-*b*-PLA-*b*-PVP triblock architecture imposes a fundamentally different topological constraint. In this case, the PLA block is confined between two hydrophilic domains and must span the micellar interior, effectively bridging the PEG- and PVP-rich hemispheres. This constraint suppresses chain coiling and biases PLA toward a more extended configuration. As a result, the characteristic dimensions of the hydrophobic domain, and consequently of the micelle, are substantially increased relative to the diblock case, even though the aggregation numbers remain comparable. Importantly, the pronounced size difference between diblock and triblock micelles cannot be rationalized in

terms of differences in chain packing density alone. Rather, it originates from a topology-induced change in the conformational statistics of the PLA block. This interpretation is fully consistent with the scattering-derived shape descriptors, the quantitative TEM analysis, and the theoretical framework linking aggregation number, chain conformation, and micelle dimensions, as detailed in the Supporting Information. In this work, we successfully synthesized a novel amphiphilic triblock copolymer designed to promote lateral phase separation within the micelle corona. The triblock structure was thoroughly characterized in solution using gel permeation chromatography and multidimensional NMR, confirming block composition and connectivity. Upon self-assembly in aqueous solution, micelle morphology was investigated by cryogenic transmission microscopy (cryoTEM), dynamic light scattering (DLS), and Guinier analysis from multi-angle light scattering, confirming the formation of asymmetrical micelles with a low degree of polydispersity. To probe the spatial arrangement of the hydrophilic blocks within the corona, we employed unstained TEM and an iridium-labeled PVP chain end. The resulting micelles exhibited clear contrast asymmetry, directly visualizing the confinement of the PVP block to one hemisphere. Complementary 2D ^{1}H-NOESY experiments revealed an absence of cross-peaks between PEG and PVP segments, supporting a laterally segregated corona structure. Together, these findings provide strong evidence for the formation of Janus-type micelles and pave the way for further research toward the development of hydrophilic, biocompatible, polymer-based Janus nanoparticles with dual functionality and broad application potential, ranging from advanced catalysis to targeted nanomedicine.

Acknowledgments

Funding for this research was provided by the following: EXCELLENT SCIENCE—European Research Council grant (CheSSTaG 769798 (G.B.)), the European Union (ERC-2023-POG, MAIN, 101123468) (G.B.), the Ministerio de Ciencia e Innovación (PID2020-119914RB-I00 (G.B.), PID2023-149206OB-I00 (G.B.), and PID2022-138109OB-I00 (L.R.P.)), the Alzheimer's Association Research Grant—New to the Field (AARG-NTF): 23AARG-NTF-1027312 (G.B.), the Agència de Gestió d'Ajuts Universitaris i de Reserca grant 2021 SGR 01538 (G.B.), and European Union NextGenerationEU—Biotechnology Complementary Plan Applied to Health ADNano PRTR-C17.I1; PRTR-C17.I01.P01.S13 (AAAA_ACG_AY_2539/22_05) (G.B.) and the National Key R&D Program of China (2022YFC2009900) (X.T.).

Conflicts of Interest

The authors declare no conflicts of interest.

Data Availability Statement

The data that support the findings of this study are available in the Supporting Information of this article.

References

1. H. Su, C. Hurd Price, L. Jing, Q. Tian, J. Liu, and K. Qian, "Janus Particles: Design, Preparation, and Biomedical Applications," *Materials Today Bio* 4 (2019): 100033.

2. A. Walther and A. Müller, "Janus Particles: Synthesis, Self-Assembly, Physical Properties, and Applications," *Chemical Reviews* 113, no. 7 (2013): 5194–5261.

3. A. Walther, C. Barner-Kowollik, and A. H. E. Müller, "A Systematic Study of Thermoresponsive Bis-Hydrophilic Block Terpolymers," *Langmuir* 26, no. 14 (2010): 12237–12246.

4. M. Charlaganov, O. Borisov, and F. Leermakers, "Modeling of Triblock Terpolymer Micelles With a Segregated Corona," *Macromolecules* 41, no. 10 (2008): 3668–3677.

5. J. Du and S. Armes, "Patchy Multi-Compartment Micelles are Formed by Direct Dissolution of an ABC Triblock Copolymer in Water," *Soft Matter* 6, no. 19 (2010): 4851–4857.

6. T. Liu, C. De Pace, R. Huang, et al., "An Iridium (III) Complex Revealing Cytoskeleton Nanostructures Under Super-Resolution Nanoscopy and Liquid-Phase Electron Microscopy," *Sensors and Actuators B: Chemical* 388 (2023): 133839.

7. J. Lutz, H. Börner, and K. Weichenhan, "Combining ATRP and "Click" Chemistry: A Promising Platform Toward Functional Biocompatible Polymers and Polymer Bioconjugates," *Macromolecules* 39, no. 19 (2006): 6376–6383.

8. A. J. de Graaf, E. Mastrobattista, C. F. van Nostrum, D. T. S. Rijkers, W. E. Hennink, and T. Vermonden, "ATRP, Subsequent Azide Substitution and 'Click' Chemistry: Three Reactions Using One Catalyst in One Pot," *Chemical Communications* 47, no. 24 (2011): 6972–6974.

9. L. Zhang and A. Eisenberg, "Multiple Morphologies of "Crew-Cut" Aggregates of Polystyrene-b-poly(acrylic acid) Block Copolymers," *Science* 268, no. 5218 (1995): 1728–1731.

10. L. Ruiz-Pérez, L. Messager, J. Gaitzsch, et al., "Molecular Engineering of Polymersome Surface Topology," *Science Advances* 2, no. 4 (2016): e1500948.

11. A. Blanazs, M. Massignani, G. Battaglia, S. P. Armes, and A. J. Ryan, "Tailoring Macromolecular Expression at Polymersome Surfaces," *Advanced Functional Materials* 19, no. 18 (2009): 2906–2914.

12. G. Battaglia and A. Ryan, "Bilayers and Interdigitation in Block Copolymer Vesicles," *Journal of the American Chemical Society* 127, no. 24 (2005): 8757–8764.

13. J. Muñoz-López, G. M. Tuveri, V. Barbieri, et al., "Decoding the Conformation of Lactic Acid in Block Copolymer Micelles," *Journal of the American Chemical Society* 148 (2026): 4839–4843.

14. H. Mertens and D. Svergun, "Structural Characterization of Proteins and Complexes Using Small-Angle X-Ray Solution Scattering," *Journal of Structural Biology* 172, no. 1 (2010): 128–141.

15. J. Tants and A. Schlundt, "Advances, Applications, and Perspectives in Small-Angle X-Ray Scattering of RNA," *ChemBioChem* 24, no. 17 (2023): e202300110.

16. N. Sheveleva, P. V. Konarev, K. M. Boyko, et al., "SAXS, DLS, and MD Studies of the Rg/Rh Ratio for Swollen and Collapsed Dendrimers," *Journal of Chemical Physics* 161, no. 19 (2024): 194901.

17. I. K. Voets, R. Fokkink, T. Hellweg, et al., "Spontaneous Symmetry Breaking: Formation of Janus Micelles," *Soft Matter* 5, no. 5 (2009): 999–1005.

18. I. K. Voets, A. de Keizer, M. A. Cohen Stuart, and P. de Waard, "Core and Corona Structure of Mixed Polymeric Micelles," *Macromolecules* 39, no. 17 (2006): 5952–5955.

19. I. K. Voets, A. de Keizer, P. de Waard, et al., "Double-Faced Micelles From Water-Soluble Polymers," *Angewandte Chemie International Edition* 45, no. 40 (2006): 6673–6676.

20. R. López-Rios de Castro, R. M. Ziolek, M. B. Ulmschneider, and C. D. Lorenz, "Therapeutic Peptides are Preferentially Solubilized in Specific Microenvironments Within PEG-PLGA Polymer Nanoparticles," *Nano Letters* 24, no. 6 (2024): 2011–2017.

Supporting Information

Additional supporting information can be found online in the Supporting Information section.

Supporting File 1: anie71403-sup-0001-SuppMat.pdf.